National Conference on Recent Trends in Synthesis and Characterization of Futuristic Material in Science for the Development of Society
(NCRDAMDS-2018)
In association with
International Journal of Scientific Research in Science and Technology

Structural and Dielectric Properties of Multiferroic $90BiFeO_3$-$10BaTiO_3$ Ceramics Synthesized by Sol-Gel

Rajesh R. Raut*1, Chandrakant S.Ulhe2
*1Science and Humanities Department, Sanmati Engineering College, SGB Amravati University, Amravati, Maharashtra. India
2Departmen Department of Physics, Yashvantrao Chavan Arts and Science SGB Amravati University, Amravati, Maharashtra, India

ABSTRACT

$90BiFeO_3$–$10BaTiO_3$ (90BFO–10BT) multiferroic material was synthesized by a Sol-Gel method. We have reported microstructure with the enhanced dielectric properties of multiferroic mixed-perovskite 90BFO–10BT compound by scanning electron microscopy (SEM) and conventional dielectric measurements. XRD observations showed secondary phase appearance during synthesis because of instability of Bismuth and charge fluctuation of Fe. Dielectric behavior of the 90BFO–10BT ceramics were studied at various temperature and frequency. It was also found that doping of $BiFeO_3$ by insulating $BaTiO_3$ enhanced the dielectric properties. The dielectric constant was found to be very high ($\varepsilon_r' = 10^2$, for T = 140°C). The Maxwell–Wagner type relaxation in the sample results a considerably high dielectric constant in 90BFO–10BT ceramics.

Keywords: Ceramic, Sol-Gel, Dielectric, XRD, SEM

I. INTRODUCTION

Multiferroic materials in which (anti-) ferroelectricity, (anti-) ferromagnetism and ferroelasticity coexist simultaneously and have gained much attention because of their wide applications in advanced technologies [1,2]. These multiferroic materials have been used in the non-volatile memory, sensors, waveguides, modulators, switches, phase invertors, rectifiers, etc [3–6].

Bismuth ferrite $BiFeO_3$ (BFO) has a rhombohedral symmetry (R3C) with a distorted perovskite structure and shown multiferroic behaviour at room temperature. Bulk $BiFeO_3$ ceramic possesses a ferroelectric Curie temperature (T_C) of 1103 K (830 ℃) and an antiferromagnetic Neel temperature (T_N) of 643 K (370 ℃) [3, 7, 8]. But the use of $BiFeO_3$ & $BiFeO_3$ based materials in technology is somewhat limited due to the low electrical resistivity & appearance of considerable concentration of impurity in these materials.

It is difficult to prepare bulk pure $BiFeO_3$ without traces of impurities. Sosonowska et al. [9] have prepared $BiFeO_3$ in the bulk form by the method used by Achenbach et al. [10], but reported a few traces of $Bi_2Fe_4O_9$. Tabares-Munoz et al. [11] also found a mark of $Bi_{46}Fe_2O_{72}$ impurity in final compound. This difficulty can be solved by forming the complex of BiFeO3 with other ceramic materials, such as $BaTiO_3$ (BT) and $PbTiO_3$ [12–14]. A pervoskite $BiFeO_3$ forms a solid solution with insulating $BaTiO_3$ (BT). As both the materials have same structure, the complex of BFO with BT have resulted in improvement of the overall electrical, ferroelectric properties & stabilizing the perovskite structure [15-24].

It is also shown by Roginskaya et al [25] that $BiFeO_3$ has low values of dielectric constant. In ferroelectric materials, the analysis of dielectric variation becomes difficult [26]. The high dielectric loss for high temperatures is resolved by Krainiket al [27] by analysing the temperature dependence of dielectric constant of $BiFeO_3$ at lower frequencies. Smith et al. [28] used other perovskite materials as a dopant to make $BiFeO_3$ an highly resistive. They synthesized the mixture of $BiFeO_3$–$PbTiO_3$ with high values of resistivity and low dielectric losses. Analysing the Curie temperature T_C for different compositions, they exactly

calculated the transition temperature of the pure sample. Literature review shows that $BiFeO_3$ shows changes in structure, when it forms solid solutions with other perovskite materials such as $BaTiO_3$. Also the content of the secondary phase is found to be increased. The structure is found to be rhombohedral for the concentration of 100 and 67 mol% and exhibited tetragonal structure below 7.5 mol% of $BiFeO_3$ [29]. Due to these structural changes resulted significant variation in the dielectric and magnetic properties [30].

These shows that dielectric/magnetic properties are dependent on the structural changes in (1-x) BFO–(x) BT [31–33]. This paper reported the results on structural and dielectric, impedance properties of $90BiFeO_3$–$10BaTiO_3$ (90BFO–10BT) ceramics. Emphasis is given to find the cause of high dielectric constant in 90BFO-10 BT ceramics using dielectric spectroscopy.

II. METHODS AND MATERIAL

For Synthesis of 90BFO–10BT ceramics, first, $BiFeO_3$ powder is prepared by using a method mentioned somewhere. [34] In order to obtained a ceramics of 90BFO–10BT, powder form $BaTiO_3$ (Sigma-Aldrich, purity > 99.9 %) is mixed with BFO in proportion amount with the help of agate mortar and pestle. The homogeneous fine mixture of this composition is obtained by ball milling for 24 h. Then, the pellet, which are prepared with the help of uniaxial hydraulic press are sintered at 870 °C /**4** h. The above prepared sintered pellets were analysed for their structural properties using XRD technique. Surface morphology was studied using scanning electron microscope (SEM) (Jeol JSM-7600F).

Dielectric measurements were done by using Novocontrol broadband dielectric spectrometer (Alpha A analyzer Novocontrol GmbH, with BDS 1200 sample holder), in the frequency and temperature range of 1 Hz to 1 MHz and 0 – 350 °C respectively.

III. RESULTS AND DISCUSSION

A. Phase and Microstructure detection of 90BFO–10BT Ceramic

The powder XRD pattern of 90BFO–10BT sintered at 870 °C is shown in Figure 1.

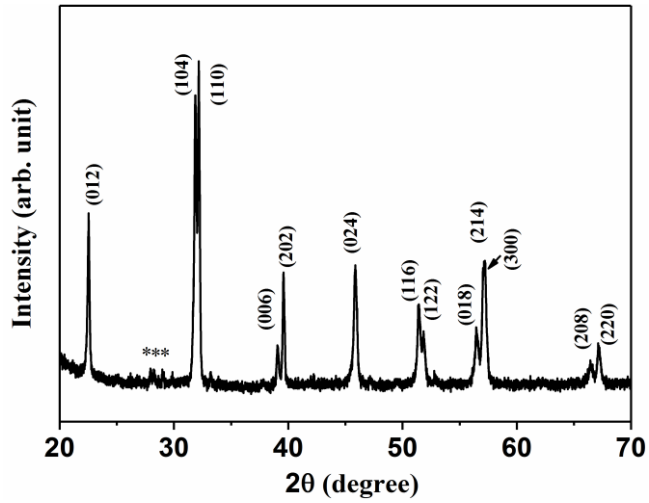

Figure 1. Powder X-ray diffraction pattern of 90BFO–10BT ceramics

The XRD pattern shows distorted rhombohedral system of 90BFO–10BT due to the addition of BT to BFO. The structure has been identified using JCPDS file (01-086-1518). The structure exhibit R3C space group with the lattice parameter a = 5.58 Å and c = 13.8670 Å.

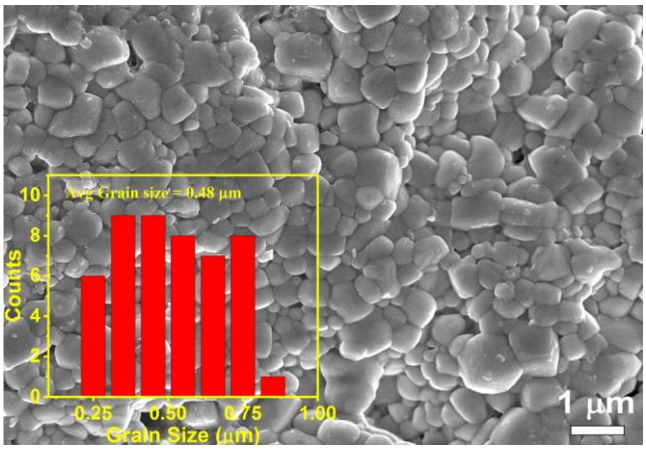

Figure 2. Scanning Electron Micrograph of pure 90BFO–10BT ceramic

However, there were minute traces of $Bi_2Fe_4O_9$ which we believe is not going to interfere in any of the measurements. The remarkable diffraction peak at 32.08° may be due the diffraction from the <110> plane. Further, it can be confirmed that the solid solution of BFO and BT can be formed, as no marks of $BaTiO_3$ is visible from XRD pattern.

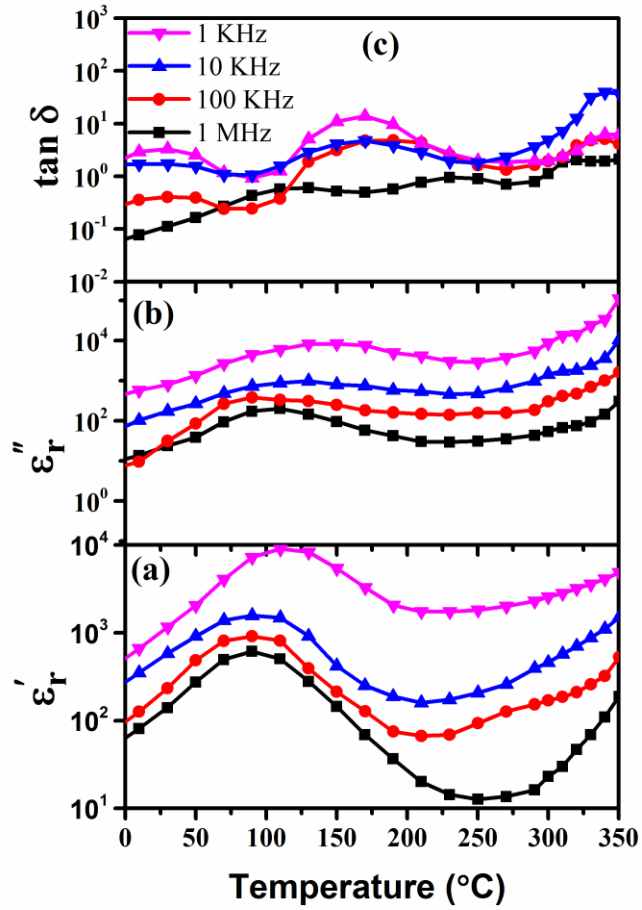

Figure 3. (a) Real part of dielectric constant (b) Imaginary part of dielectric constant and (c) dielectric loss (tan δ) as a function of temperature at different frequencies for 90BFO–10BT ceramics.

Figure 2 shows SEM image of 90BFO-10BT synthesized by Sol-Gel. The average grain size of the sample sintered at 870 °C /**4** h is found to be submicron sized (≤ 0.48 μm). SEM image revealed a dense microstructure & uniform grain distribution. This improvement in the density of BFO by the formation of more uniform grains in the ceramic matrix is because Ba^{2+} and Ti^{4+} acts as a A- and B-site substituent in the ABO_3 perovskite structure.

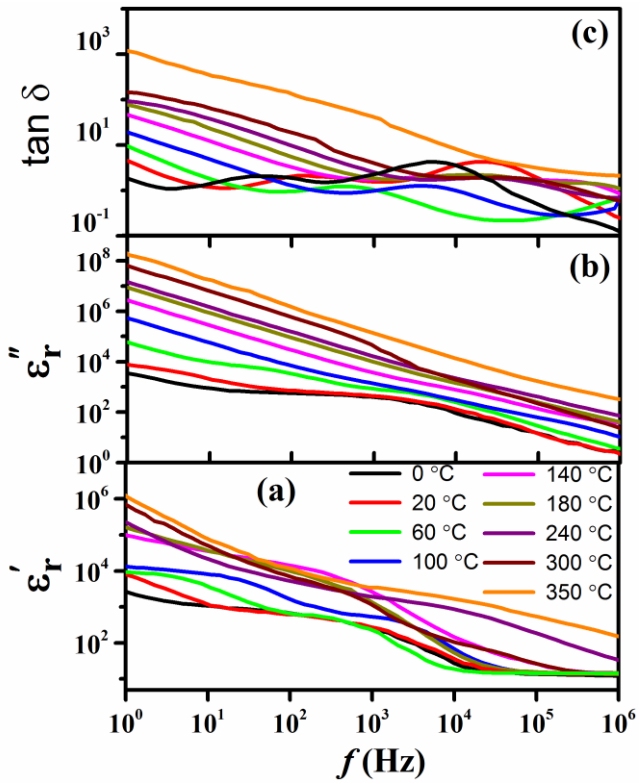

Figure 4. (a) Real part of dielectric constant (b) Imaginary part of dielectric constant and (c) dielectric loss (tan δ) as a function of frequency for different temperature of 90BFO–10BT ceramics.

B. Dielectric Behaviour of 90BFO–10BT Ceramic

(i) Temperature Dependence Dielectric Properties of 90BFO–10BT Ceramics

Figure 3 shows the temperature (0 – 350 °C) dependence of dielectric properties of 90BFO–10BT ceramics at a frequency of 1 Hz, 10 KHz and 100 KHz. At 25^0C temperature, the dielectric constant and dielectric loss was found to be > 120 and > 0.5 at 100 kHz respectively, which is higher than BFO samples reported earlier [35]. This is attributed by the space charges and grain boundary effect. The high dielectric constant (ε_r' > 5 X 10^2, for f < 10 MHz) and low loss (tan δ ≤ 1, f > 10 KHz) are observed on temperature range (0 – 350 °C) for the sample. A characteristic step-like decrease in ε_r' is also observed in dielectric behaviour shown in figure 3.

Also a broad relaxation peak (in tan δ) with an increase in temperature is observed for (ε_r') at around 100 – 150 °C. This peak in dielectric constant is considerably close to the magnetic transition temperature of BFO which shows the magnetic-electric coupling of 90BFO–10BT. These two concepts closeness to T_N and presence

of two valence states Fe^{2+} and Fe^{3+} in $BiFeO_3$, resulted in the dielectric relaxation peaks and improvement in the dielectric properties.

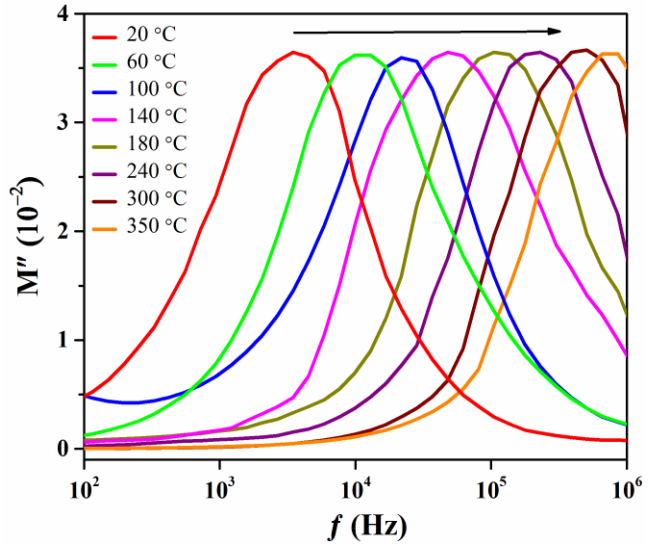

Figure 5. Imaginary part of modulus at a few discrete temperatures for 90BFO–10BT ceramic.

(i) Frequency Dependence Dielectric Properties of 90BFO–10BT Ceramics

Figure 4 (a) shows the dielectric (ε_r') properties of 90BFO–10BT ceramics with frequency. High values of $\varepsilon_r' > 10^2$ for T > 60 °C found for 90BFO–10BT. The space charge polarization effects results in high value of ε_r' (> 10^3) which is observed at lower frequencies (<100 Hz). This effect does not take place at higher frequencies (>100 Hz). The steady decrease in ε_r' with frequency is observed that may be due to the lack of dipoles ability created at interfaces to arrange themselves to the externally applied frequencies. A sharp decrease in ε_r' which iappears to be shifting towards the higher frequency is due to the Maxwell–Wagner type relaxation process take place in the sample. Corresponding to this sharp fall in ε_r', there exist a peak in the ε_r'' versus frequency graph.

From Figure 4(b), the variation of ε_r'' with slope of -1 infer the dc conductivity which plays a major role for dielectric losses in the sample. This can be represented by [36]

$$\varepsilon'' = \sigma_{dc} / \omega \varepsilon_o$$

where, σ_{dc} is the dc conductivity sample and ε_o is the permittivity of free space.

Figure 5 shows the modulus plot versus frequency at temperatures from 20 °C to 350 °C. Peaks in graph for sintered 90BFO-10BT shows the hopping mechanism which is strongly dependant on temperature.

IV. CONCLUSION

In the present work, 90BFO–10BT ceramics with high dielectric constant & dielectric loss were synthesized by sol–gel method. XRD clearly indicates the distorted rhombohedral structure of sample sintered at 870 °C/4h. SEM confirms the formation of pure and dense 90BFO–10BT ceramics with the average grain size of 0.48 μm. Remarkably high values ($\varepsilon_r' > 5$ X10^2 for f < 10 MHz) and low loss (tan $\delta \leq 1$, for f > 10 KHz) were observed for the temperature range (0 – 350 °C) for the sample. The high dielectric constant could be well explained on the basis of Maxwell–Wagner response and hopping process of charge carriers between Fe^{2+} and Fe^{3+} valence states of Fe. The modulus spectroscopic plot indicates the temperature dependent hopping mechanism. The complex impedance study at different temperatures indicates the increase in AC conductivity.

In all, the addition of BT into BFO reduces the dielectric losses and increases the resistive property of the 90BFO-10BT, which gives outstanding technological importance to 90BFO-10BT ceramic.

V. ACKNOWLEDGMENTS

We would like to thank Department of Metallurgical Engineering and Materials Science, CRNTS of IIT Bombay for providing the characterization facilities viz. XRD, SEM, Dielectric, etc.

VI. REFERENCES

[1]. N. Fujimura, S. Azuma, N. Aoki, T. Yoshimura and T. Ito: J. Appl. Phys. (1996) 80,7084.

[2]. N. Fujimura, T. Ishida, T. Yoshimura and T. Ito: Appl. Phys. Lett. (1996) 69,1011

[3]. T. Shao, A. Scholl, F. Zavaliche, K. Lee, M. Barry, A. Doran, M.P. Cruz, Y.H. Chu, C. Ederer, N.A., Spaldin, R.R. Das, D. M. Kim, S.H. Baek, C.B. Eom, R. Ramesh, Nature Materials(2006) 5 , 823-829.

[4]. H. Fukumura, S. Matsui, N. Tonari, T. Nakamura, N. Hasuike, K. Nishio, T. Isshiki, H. Harima, K.

Kisoda, Acta Physica Polonica A (2009) 116, 47-50.
[5]. A.Z. Simoes, A.H.M. Gonzalez, L.S. Cavalcante, C.S. Riccardi, E. Longo, J.A. Varela, Journal of Applied Physics (2007) 101, 1-6 074108.
[6]. V.A. Khomchenko, D.A. Kiselev, M. Kopcewicz, M. Maglione, V.V. Shvartsman, P. Borisov, W. Kleemann, A.M.L. Lopes, Y.G. Pogorelov, J.P. Araujo, R.M. Rubinger, N.A. Sobolev, J.M. Vieira, A.L. Kholkin, Journal of Magnetism and Magnetic Materials (2009),321, 1692-1698.
[7]. S.V. Kiselev, R.P. Ozerov, G.S. Zhdanov, Sov. Phys. Dokl. (1963) 7, 742.
[8]. P. Fischer, M. Polomska, I. Sosnowska, M. Szymanski, J. Phys. (1980) C 13, 1931.
[9]. I. Sosonowska, T. Peterlin-Neumaier, and E. Steichele,J. Phys. (1982), C15, 4835.
[10]. G.D. Achenback, W.J. James,andR. Gerson, J. Amer. Ceram. Soc. (1967) 50, 437.
[11]. C. Tabares-Munoz, J.P. Rivera, A. Bezinges, A. Monnhier, and H. Schmid, Jpn. J. Appl. Phys. (1985) 24, 24.
[12]. R. Rai, I. Bdikin, M.A. Valente, A.L. Kholkin, Materials Chemistry and Physics (2010) 119, 539-545.
[13]. R.A.M. Gotardo, I.A. Santos, L.F. Co ´tica, E.R. Botero, D. Garcia, J.A. Eiras, Scripta Materialia (2009) 61,508-511.
[14]. W. Sakamoto, A. Iwata, M. Moriya, T. Yogo, Materials Chemistry and Physics (2009) 116, 536-541
[15]. M.M. Kumar, A. Srinivas, S.V. Suryanarayana, J. Appl. Phys. (2000) 87, 855.
[16]. M.T. Buscaglia, L. Mitoseriu, V. Buscaglia, I. Pallecchi, M. Viviani, P. Nanni, A.S. Siri, J. Eur. Ceram. Soc. (2006)26, 3027.
[17]. R. Rai, I. Bdikin, M.A. Valente, A.L. Kholkin, Mater. Chem. Phys. (2010) 119, 539.
[18]. R.A.M. Gotardo, I.A. Santos, L.F. Co´tica, E.R. Botero, D. Garcia, J.A. Eiras, Scr. Mater. (2009) 61, 508.
[19]. S.O. Leontsev, R.E. Eitel, J. Am. Ceram. Soc. (2009) 92, 2957.
[20]. C. Zhou, H. Yang, Q. Zhou, G. Chen, W. Li, H. Wang, J. Mater. Sci.: Mater. Electron. (2013) 24, 1685.
[21]. H.Y. Dai, J. Chen, T. Li, D.W. Liu, R.Z. Xue, H.W. Xiang, Z.P. Chen, J. Mater. Sci.: Mater. Electron. (2015)26, 3717.
[22]. M. Kumar, S. Shankar, O. Thakur, A. Ghosh, J. Mater. Sci. Mater. Electron. (2015) 26, 1427.
[23]. J. Bernard, Piezoelectric Ceramics (Academic Press, New York,(1971).
[24]. G. Arlt, D. Hennings, G. de With, J. Appl. Phys. (1985) 58, 1619.
[25]. Yu. E. Roginskaya, Yu. Ya. Tomashpol'ski, Yu. N. Venevtsev, V. M. Petrov, and G. S. Zhdanov, Sov. Phys. (1966) JETP23, 490.
[26]. I. R. Teague, R. Gerson, and W. J. James, Solid State Commun. (1970) 8, 1073.
[27]. N. N. Krainik, N. P. Khuchua, V. V. Zhdanova, and V. A. Evseev, Fiz. Tverd. Tela (S.-Peterburg) (1966) 8, 816 [Sov. Phys. Solid State].
[28]. R. T. Smith, G. D. Achenbach, R. Gerson, and W. J. James, J. Appl. Phys. (1968) 39, 70.
[29]. I.H. Ismailzade, R.M. Ismailov, A.I. Alekberov, and F.M. Salaev, phys. stat. sol. (a) (1981) 68, K81.
[30]. M.M. Kumar, A. Srinivas, S.V. Suryanarayana, J. Appl. Phys. (2000) 87, 855.
[31]. W. Li, J. Qi, Y. Wang, L. Li, Z. Gui, Mater. Lett., (2002) 57, 1.
[32]. A. Umeri, T. Kuku, N. Scuor, V. Sergo, J. Mater. Sci. (2008) 43, 922.
[33]. Y. Yuan, S. Zhang, W. You, Mater. Lett., (2004).58, 1959.
[34]. Jayant Kolte, Devidas Gulwade, Aatish Daryapurkar, Materials Science Forum, (2012) Vols 702-703 pp 1011-1014.
[35]. T. Moriya, Phys. Rev., (1960) 120, 91.
[36]. P. Salame, R. Drai, O. Prakash, A.R. Kulkarni, Ceram. Int., (2014) 40, 4491.